Sampling Phase Estimation in Underwater PPM Fractionally Sampled Equalization

Gaetano Scarano, Andrea Petroni, Roberto Cusani, Mauro Biagi
Dipartimento di Ingegneria dell'Informazione, Elettronica e Telecomunicazioni (DIET)
Università di Roma "La Sapienza"
Roma, Italy
{gaetano.scarano, andrea.petroni, roberto.cusani, mauro.biagi}@uniroma1.it

***Abstract*—A new blind estimator of the sampling phase is proposed to support fractionally spaced equalization in underwater digital links employing pulse position modulation. Stemming from the relationship between the "spikiness" of the channel impulse response and the deviation from Gaussianity of the received signal, the sampling phase is estimated by exploiting non-Gaussianity measures offered by nonlinear statistics. In particular, the fourth order (kurtosis) and the first order nonlinear sample moments are considered and the resulting receiver performance is analyzed.**

***Index Terms*—Underwater, PPM, Fractional Sampling, Channel Equalization**

I. Introduction

Intersymbol interference (ISI) represents the main impairment in wireless data links over multipath channels. Reducing ISI becomes particularly complicated in the context of underwater acoustic communications (UWAC) where attenuation, noise and multipath result in a large channel delay spread severely degrading the received signal quality [1].

The easiest way to mitigate ISI is to introduce a guard interval between consecutive emitted symbols so to avoid symbols overlapping. On the other hand, the consequent drawback is the communication rate reduction, as the presence of large *recovery* times makes the transmission essentially in stand-by. Furthermore, although this solution may be reasonable in RF-based technology, it becomes instead harmful when dealing with UWAC where the transmission rate is already *penalized by nature* as the speed of sound is five orders of magnitude lower than the speed of light.

An alternative solution to the use of guard time is represented by digital filtering after sampling at receiver side aimed at obtaining the *channel equalization* condition. However, the introduction of an efficient equalization scheme may significantly increase the receiver software/hardware complexity. This is an important aspect to take care of, since devices employed in underwater applications are quite expensive and a good trade-off between performance and computational cost is of paramount importance.

Channel equalization is necessary especially when dealing with shallow water communications where the multipath effect makes the received signal subject to strong interference. Therefore suitable techniques are requested in order to allow ISI cancellation. In this regard, the typical underwater channel selectivity can be tackled by resorting to turbo equalization, the effectiveness of which is recognized in both linear and decision feedback approaches. Turbo equalization finds use also in Multiple-Input Multiple-Output single-carrier communications as reported in [2], [3].

A remarkable part of the works in literature presents solutions based on the implementation of Decision Feedback Equalizers (DFE) [4]. This kind of nonlinear filtering is used when the signal distortion caused by the channel can not be reliably mitigated by linear equalizers. The fast convergence provided by DFEs is paid in terms of computational cost since the coefficients updating concerns two filters, instead of a single filter as in the case of linear equalization. An example of DFE applied to single-carrier UWAC is reported in [5], where an iterative frequency domain equalization combined with low density parity check (LDPC) decoding is presented.

Another key element to consider when dealing with ISI-affected communications is the proper selection of the modulation scheme to be employed. In this regard, Pulse Position Modulation (PPM) is known to be particularly robust to ISI thanks to its time-frequency properties. DFE in PPM-based communications, even though not specifically related to the underwater scenario, is introduced in [6].

As far as PPM is concerned, it is worth noting that most of works reported in the literature deal with filtering operated at chip time. This choice may lead to a not-negligible and annoying time sensitivity that, in addition to the undesired noise amplification effect, impacts on the overall system performance.

This problem can be overcome by sampling the received signal at rates greater than the nominal one before filtering. This technique is known as fractionally spaced channel equalization [7], and the resulting filter is so-called fractionally spaced equalizer (FSE) [8]. Signal oversampling to obtain accurate channel equalization is also diffused in other fields such as terrestrial digital video broadcasting services [9]. In this direction, an application of fractionally spaced equalization in the underwater con-

ISBN 978-90-827970-1-5

text is given in [10], where the authors propose an improved version of the Recursive Least Squares-Constant Modulus Algorithm (RLS-CMA) ruling a FSE. In particular, a modified cost function of the CMA is there introduced allowing both faster convergence and computational cost reduction with respect to the standard RLS-CMA. However, equalizer performance strictly depends on the initial phase the received fractionally sampled signal is locked to. In fact, the sampling phase has to be chosen among P possible ones when working with a fractional sampling factor equal to P. The *recognition* of the most suitable sampling phase allows the equalizer to reach a faster convergence, and very often to avoid misconvergence.

All the previous considerations motivated us in investigating estimation techniques of the sampling phase; in the sequel we present a novel blind estimation technique based on nonlinear statistics directly measured on the received signal.

II. MPPM Waveform

Loosely speaking, the peculiarity of MPPM signals is that each symbol is formed by M consecutive chips of which one and only one is filled with a pulse while the others are empty. The position of the filled chip encodes the transmitted information.

To gain a deeper insight about the spectral structure of PPM induced by this signal peculiarity, we will see how MPPM signals can be expressed as ***particular PAM signals modulating a sequence of suitably correlated binary samples***.

To this purpose, let us consider the n-th string $s_n = (b_{0,n}, b_{1,n}, \ldots, b_{\nu-1,n})$ collecting the $\nu = \log_2 M$ bits to be transmitted after a suitable mapping to the corresponding MPPM symbol. This mapping is operated as follows: *i)* denoting by j_n the decimal value of the binary number s_n, the j_n-th row of the identity M-matrix $\mathbf{I}_M$ furnishes a M-tuple of binary valued *chips* $(c_n[0], c_n[1], \ldots, c_n[M-1])$; *ii)* the n-th MPPM discrete symbol is formed as follows:

$$c_{M\text{PPM}}[n] = \sum_{m=0}^{M-1} c_n[m]\,\delta[n-m],\ n = 0, 1, \ldots, M-1 \quad (1)$$

The MPPM discrete symbol expression (1) properly takes into account the fully-correlation existing between the M chip samples $(c_n[0], c_n[1], \ldots, c_n[M-1])$, $M-1$ of which are equal to 0 and the remaining to 1.

Using (1), we can form a binary stochastic sequence that accounts for all the discrete symbols of a MPPM signal:

$$b_{M\text{PPM}}[n] = \sum_{k=-\infty}^{+\infty} c_{M\text{PPM}}[n - kM] \quad (2)$$

For equiprobable bits, the direct component (DC) and the power of the sequence $b_{M\text{PPM}}[n]$ are:

$$\textit{(DC)} \quad \mathcal{M}_{M\text{PPM}} = \frac{1}{M} \quad (3)$$

$$\textit{(Power)} \quad \mathcal{P}_{M\text{PPM}} = \frac{M-1}{M^2} \quad (4)$$

The analog MPPM signal is then formed by interpolating the binary sequence $b_{M\text{PPM}}[n]$ with a shaping pulse $g_{\text{T}}(t)$ whose duration equals the chip-time T_c:

$$s_{M\text{PPM}}(t) = \sum_{n=-\infty}^{+\infty} b_{M\text{PPM}}[n]\, g_{\text{T}}(t - nT_c) \quad (5)$$

Since each MPPM symbol if formed by M consecutive chips, the symbol-time is $T_s = M\,T_c$.

The form (5) is particularly interesting since it allows a relatively simple derivation of the Power Spectral Density (PSD) of the analog MPPM signal:

$$P_{s_{M\text{PPM}}}(j\Omega) = |G_{\text{T}}(j\Omega)|^2\, P_{b_{M\text{PPM}}}(e^{j\Omega T_c}) \quad (6)$$

In (6), $G_{\text{T}}(j\Omega)$ is the Fourier Transform of $g_{\text{T}}(t)$, and $P_{b_{M\text{PPM}}}(e^{j\omega})$ is the PSD of the discrete binary random sequence of the MPPM symbols $b_{M\text{PPM}}[n]$, whose expression, calculable as indicated in [13] or in a more simple fashion as indicated in [14], is:

$$P_{b_{M\text{PPM}}}(e^{j\omega}) = \frac{1}{M}\left[1 - \left|\frac{\sin(\omega M/2)}{M\sin(\omega/2)}\right|^2\right] + \frac{2\pi}{M^2}\sum_{k=-\infty}^{+\infty}\delta(\omega - 2\pi k) \quad (7)$$

As shown in Fig.1, the PSD (6) reveals the rich spectral redundancy possessed by the MPPM signal.

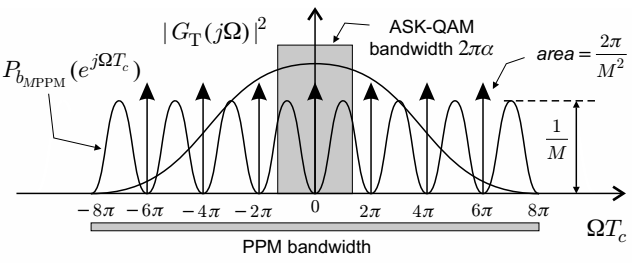

Figure 1. MPPM power spectral density.

Generally speaking, due to the large bandwidth of the pulse $g_{\text{T}}(t)$, the MPPM signal presents a sort of redundancy that consists in a special kind of spectral repetition coding. To outline the MPPM signal redundancy, in Fig.1 we have also indicated the bandwidth occupied by shaping pulse used in transmitting the chip sequence $b_{M\text{PPM}}[n]$ by Amplitude Shift Keying (ASK) or Quadrature Amplitude Modulation (QAM) techniques; we observe that also ASK-QAM realizes spectral repetition coding but only in the very small band determined by the roll-off factor α, precisely of width α/T_c around half the symbol rate $1/2T_c$.

ISBN 978-90-827970-1-5 © EURASIP 2018

We believe that Fig.1 offers a somewhat novel and interesting way to understand the well-known ISI robustness vs. transmission rate trade-off of PPM based signaling.

Moreover, since $b_{M\text{PPM}}[n]$ is a binary sequence, the MPPM signal form (5) suggests that equalization schemes developed for ASK-QAM based communications can be fruitfully employed also in MPPM based communications. In particular, in [15] we have developed a somewhat novel blind fractionally spaced equalization scheme that properly takes into account the probabilistic description of the colored sequence $b_{M\text{PPM}}[n]$.

III. MPPM Receiver

After matched filtering at receiver side we have the signal, see also Fig.2:

$$r(t) = \sum_{n=-\infty}^{+\infty} b_{M\text{PPM}}[n]\, g(t - nT_c) + (w * g_{\text{R}})(t) \quad (8)$$

where $g(t) = (g_{\text{T}} * h * g_{\text{R}})(t)$ is the overall impulse response that accounts for the matched filter $g_{\text{R}}(t) = g_{\text{T}}(-t)$ as well as the channel $h(t)$, and $w(t)$ denotes independent additive noise observed before the matched filter.

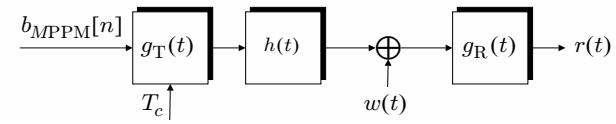

Figure 2. Chip based PPM transmission scheme.

The large bandwidth occupied by the MPPM signal, see Fig.1, can be usefully exploited through fractional sampling of $r(t)$ operating at rate P/T_c, where the fractional sampling integer factor P can assume values significantly greater than 1; for instance, the numerical results later presented in Sect.V have been obtained using $P = 9$.

As depicted in Fig.3, a FSE is a digital filter that operates on samples of $r(t)$ taken at rate P/T_c, while yielding outputs at rate $1/T_c$; indicating with $f[k]$ the impulse response of a FIR FSE of order L, the binary MPPM equalized sequence is:

$$\hat{b}[n] = \sum_{k=0}^{L} f[k]\, r(nT_c - kT_c/P - k_0 T_c/P) \quad (9)$$

In (9), k_0 denotes the sampling phase and takes value in the set $\mathbb{N}(P) = \{0, 1, \ldots, P-1\}$.

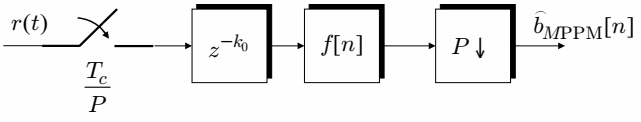

Figure 3. Chip based fractionally spaced equalization.

The following remarks are in order:

1) the choice of k_0 is not obvious;
2) different values of k_0 lead to different fractionally sampled overall channel impulse responses $g((k-k_0)T_c/P)$, so the "difficulty" encountered by any FSE, and the consequent performance loss, is significantly influenced by k_0;
3) the success of a ***blind FSE*** is almost entirely due to an opportune choice of k_0.

IV. Blind Fractional Sampling Phase Estimation

In the following, the problem of fractional sampling phase k_0 estimation is addressed. In detail, the goal is to recognize the phase k_0 that maximizes the ***spikiness*** of the fractionally sampled overall channel impulse response $g((k-k_0)T_c/P)$. In fact, spikiness simply means that $g((k-k_0)T_c/P)$ exhibits a relatively small number of large coefficients and it is expected that the chances of channel equalization grow as the channel spikiness becomes more marked.

The estimation technique here developed is ***blind*** since it directly operates on the received samples $r((k-k_0)/T_c)$ without any knowledge about the channel impulse response $h(t)$. Stemming from the convolution summation in (8), the following consideration is in order: ***the more the spikiness of the deterministic sequence*** $g((k-k_0)T_c/P)$, ***the more the deviation from Gaussianity of the stochastic sequence*** $r((k-k_0)T_c/P)$. Then, spikiness and non-Gaussianity go hand in hand, and any measures of non-Gaussianity of $r((k-k_0)/T_c)$ can be taken as a measure of spikiness of $g((k-k_0)T_c/P)$.

Here we have considered two nongaussianity measures offered by suitable NonLinear Statistics (NLS) calculated through sample averaging of N observed samples $r((k-k_0)T_c/P)$, specifically:

fourth order (sample kurtosis):

$$\mathcal{K}(k_0) = \frac{\frac{1}{N}\sum_{k=0}^{N-1} r^4\left(\frac{(k-k_0)T_c}{P}\right)}{\left[\frac{1}{N}\sum_{k=0}^{N-1} r^2\left(\frac{(k-k_0)T_c}{P}\right)\right]^2} - 3$$

first order:

$$\mathcal{S}(k_0) = \frac{\frac{1}{N}\sum_{k=0}^{N-1} \left| r\left(\frac{(k-k_0)T_c}{P}\right)\right|}{\left[\frac{1}{N}\sum_{k=0}^{N-1} r^2\left(\frac{(k-k_0)T_c}{P}\right)\right]^{\frac{1}{2}}}$$

The estimation of the fractional sampling phase is conducted as follows:

$$\hat{k}_0^{(\mathcal{K})} = \arg \min_{k_0 \in \mathbb{N}(P)} \mathcal{K}(k_0) \quad (10)$$

$$\hat{k}_0^{(\mathcal{S})} = \arg \max_{k_0 \in \mathbb{N}(P)} \mathcal{S}(k_0) \quad (11)$$

ISBN 978-90-827970-1-5 © EURASIP 2018

V. Numerical Results

Numerical results refer to the typical underwater multipath channel as that one used in [16], whose parameter values are found in Tab.I:

$$h(t) = \sum_{k=0}^{7} A_k \, \delta(t - \tau_k) \qquad (12)$$

In [16] the channel (12) is used in the band of width 8kHz around the center frequency $f_0 = 4$kHz, so that we have employed the following band-pass transmitting pulse with a bell shaped envelope:

$$g_T(t) = A \exp(-t^2/2\beta^2) \, (\cos(2\pi f_0 t) - \sin(2\pi f_0 t))$$

The value $\beta = T_c/4$ fixes the pulse duration to be approximatively equal to T_c and at the same time fixes the bandwidth $B \simeq 8/T_c$, so that $T_c = 1$ms yields just $B = 8$kHz.

The fractional sampling factor has been chosen equal to $P = 9$, *i.e.* the minimum one that still allows to fully exploit the spectral redundancy offered by the MPPM signal. In the case $M = 2$, Figs.4 and 5 show the three best values $\mathcal{S}(k_0)$ and $\mathcal{K}(k_0)$ measured with $N = 5120$ and calculated over 100 independent MonteCarlo runs.

We observe that the sample kurtosis yields $\hat{k}_0^{(\mathcal{K})} = 5$ with frequency 88%, while the first order sample moment yields $\hat{k}_0^{(\mathcal{S})} = 5$ with frequency 61%; moreover, the best three values obtained by the sample kurtosis are concentrated around the best one $\hat{k}_0^{(\mathcal{K})} = 5$, while this occurrence is not verified when using the first order sample moment. The compactness shown by sample kurtosis estimation makes it preferable since, as observed in [15], blind fractionally spaced equalization is generally very sensitive with respect to the sampling phase choice.

This result has been returned also when considering the same multipath channel (12), but now further smoothed by the convolution with a Hamming window of duration $8.\overline{3}$ms. The estimates obtained in this more challenging, from the equalization point of view, scenario are shown in Figs.6 and 7.

For the same channel analyzed in Figs.6-7 we observed the misconvergence rates reported in Tab.II.

As said before, the choice of the sampling phase can severely affect the performance of blind FSEs. In particular, we have implemented the fractional scheme depicted in Fig.3 in a blind fashion using the well know Constant Modulus Algorithm (CMA) [17],[18],[19].[1]

[1]CMA belongs to the more general class of Bussgang equalization algorithms [20], so-called because of convergence is reached when the equalized sequence satisfies the Bussgang invariance property [21]; generalization of Bussgang invariance are found in [22], [23].

Table I
Multipath channel parameters.

k	A_k	τ_k (ms)
0	0.808	0
1	1.0	18.6
2	0.796	30.0
3	0.461	59.3
4	0.522	61.0
5	0.831	62.9
6	0.421	91.3
7	0.725	107.9

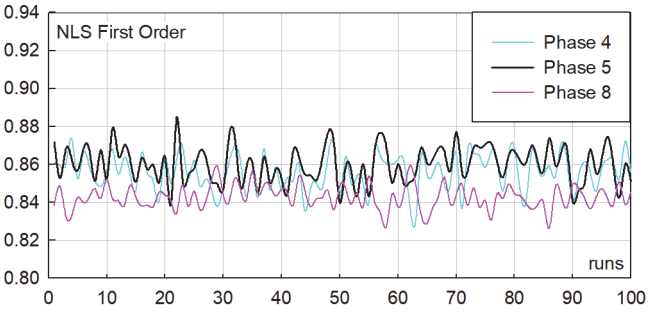

Figure 4. The three best $\mathcal{S}(k_0)$ values obtained for to $k_0 = 4, 5, 8$.

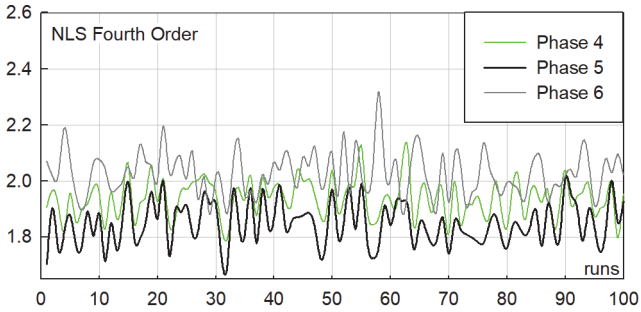

Figure 5. The three best $\mathcal{K}(k_0)$ values obtained for to $k_0 = 4, 5, 6$.

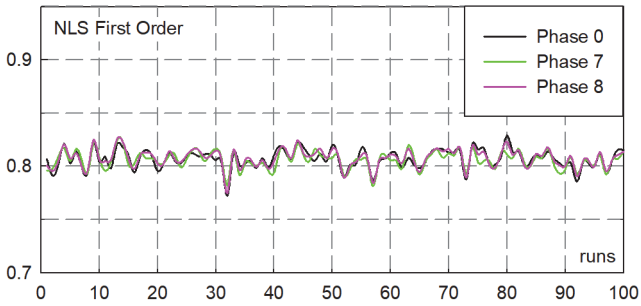

Figure 6. The three best $\mathcal{S}(k_0)$ values obtained for to $k_0 = 0, 7, 8$.

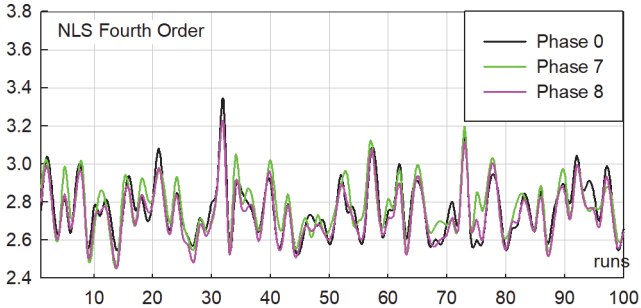

Figure 7. The three best $\mathcal{K}(k_0)$ values obtained for to $k_0 = 0, 5, 8$.

ISBN 978-90-827970-1-5 © EURASIP 2018

In this case sample kurtosis yields $\hat{k}_0^{(\mathcal{K})} = 7, 8, 0$ respectively with frequencies 24%, 44%, 30%, *i.e.* only the 2% of the times a different sampling phase is selected; on the other hand, the first order sample moment selects $\hat{k}_0^{(\mathcal{S})} = 7, 8, 0$ respectively with frequencies 16%, 28%, 21%, *i.e.* the 35% of the times a different sampling phase is recognized to be the best one.

Table II
MISCONVERGENCE PERCENTAGE OBSERVED IN CMA BASED FRACTIONALLY SAMPLED EQUALIZATION.

k_0	misconvergence percentage
7	15%
8	11%
0	5%

The results shown in Tab.II indicate that more robust blind FSE cost functions shall be investigated to deal with the equalizer sensitivity to the sampling phase choice.

VI. CONCLUSION

In this contribution a novel blind estimation technique of the sampling phase that drives a fractionally spaced equalizer operating in *M*PPM based digital transmission scenarios has been presented. Specifically, stemming from the equivalence *spiked-channel/non-Gaussian-signal*, the sampling phase can be selected using non-Gaussianity measures offered by nonlinear statistics.

In particular, two nonlinear sample moments have been considered and numerically analyzed, namely the fourth order (kurtosis) and the first order ones.

Numerical results have shown that the kurtosis based estimation is robust because the estimated sampling phase is selected within a set of three consecutive values; such a behavior is very important since the performance of blind fractionally spaced equalizers is severely affected by the choice of the sampling phase.

REFERENCES

[1] M. Stojanovic, J. Preisig, "Underwater acoustic communication channels: Propagation models and statistical characterization," *IEEE Communications Magazine*, vol.47, no.1, pp.84-89, Jan. 2009.

[2] Y.R. Zheng, J. Wu, C. Xiao, "Turbo equalization for single-carrier underwater acoustic communications", *IEEE Communications Magazine*, vol.53, no.11, pp.79-87, Nov. 2015.

[3] Z. Chen, J. Wang, Y.R. Zheng, "Frequency-Domain Turbo Equalization With Iterative Channel Estimation for MIMO Underwater Acoustic Communications", *IEEE Journal of Oceanic Engineering*, vol.42, no.3, pp.711-721, July 2017.

[4] J.G. Proakis, "Adaptive equalization techniques for acoustic telemetry channels," *IEEE Journal of Oceanic Engineering*, vol.16, no.1, pp.21-31, Jan. 1991.

[5] S. Zhao, X. Zhang, and X. Zhang, "Iterative frequency domain equalization combined with LDPC decoding for single-carrier underwater acoustic communications," in *OCEANS 2016 MTS/IEEE Monterey*, pp.1-5, Sept. 2016.

[6] A.G. Klein, C.R. Johnson, "MMSE decision feedback equalization of pulse position modulated signals," in *2004 IEEE International Conference on Communications (IEEE Cat. No.04CH37577)*, vol.5, pp.2648-2652, June 2004.

[7] G. Ungerboeck, "Fractional tap-spacing equalizer and consequences for clock recovery in data modems," *IEEE Trans.Comm.*, vol.24, no.8, pp.856-864, Aug.1976.

[8] G. Scarano, A. Petroni, M. Biagi, R. Cusani, "Second-order statistics driven LMS blind fractionally spaced channel equalization," *IEEE Signal Processing Letters*, vol.24, no.2, pp.161-165, Feb. 2017.

[9] F. Zabini, G. Pasolini, O. Andrisano, "Design Criteria for FIR-Based Echo Cancellers", *IEEE Transactions on Broadcasting*, vol.62, no.3, pp.562-578, Sept. 2016.

[10] Y. Xiao, "Recursive least squares fractionally-spaced blind equalization algorithm for underwater acoustic communication," *Journal of Information & Computational Science*, vol.10, pp.6077-6084, Dec.2013.

[11] D.J. Artman, S. Chari, R.P. Gooch, "Joint equalization and timing recovery in a fractionally-spaced equalizer," in *1992 Conference Record of the Twenty-Sixth Asilomar Conference on Signals, Systems and Computers*, vol.1, pp.25-29, Oct. 1992.

[12] A.A. Nasir, S. Durrani, R.A. Kennedy, "Blind fractionally spaced equalization and timing synchronization in wireless fading channels," *2nd Int. Conf. Future Computer and Communication*, vol.3, pp.V3-15-V3-19, May 2010.

[13] E. Biglieri, E. Benedetto, "Principles of Digital Transmission", Springer US, 1999.

[14] G. Scarano, "Lezioni di Elaborazione Statistica dei Segnali (Vol.II)", *https://www.amazon.it/Elaborazione-Statistica-dei-Segnali-vol-II/dp/1549794752*, 2018.

[15] G. Scarano, A. Petroni, R. Cusani, M. Biagi, "Blind Fractionally Spaced Channel Equalization of Underwater PPM Digital Communications Links", *submitted for publication to IEEE Trans. Wireless Communications*, available at **http://infocom.diet.uniroma1.it/gscarano/EUSIPCO2018/PPM.SP.pdf**.

[16] S. Zhao, X. Zhang, X. Zhang, "Iterative frequency domain equalization combined with LDPC decoding for single-carrier underwater acoustic communications", *MTS/IEEE OCEANS* , Monterey(CA), USA, 2016.

[17] D.N. Godard, "Self-recovering equalization and carrier tracking in two-dimensional data communications systems", *IEEE Trans. Comm.*, vol.COM-28, pp.1867-1875, Nov. 1980.

[18] G. Jacovitti, G. Panci, G. Scarano, "Bussgang-zero crossing equalization: an integrated HOS-SOS approach", *IEEE Transactions on Signal Processing*, vol.48, no.12, pp.2798-2812, Dec. 2001.

[19] G. Panci, S. Colonnese, P. Campisi, G. Scarano, "Fractionally spaced Bussgang equalization for correlated input symbols: a Bussgang approach", *IEEE Transactions on Signal Processing*, vol.52, no.5, pp.1860-1869, May 2005.

[20] S. Bellini, "Bussgang techniques for blind deconvolution and equalization", in Blind Deconvolution, S. Haykin (Ed.), Prentice Hall, pp.8-59, 1994.

[21] R. Godfrey, F. Rocca, "Zero memory non-linear deconvolution", *Geophys. Pros,*, vol.29, pp.189-228, 1981.

[22] G. Scarano, "Cumulant series expansion of hybrid non-linear moment of complex random variables", *IEEE Transactions on Signal Processing*, vol.39, no.4, pp.291-297, Apr. 1991.

[23] G. Scarano, D. Caggiati, G. Jacovitti, "Cumulant series expansion of hybrid nonlinear moments of n variates", *IEEE Transactions on Signal Processing*, vol.41, no.1, pp.486-489, Jan.1993.

ISBN 978-90-827970-1-5